Operational Implementation of the ISBA Land Surface Scheme in the Canadian Regional Weather Forecast Model. Part II: Cold Season Results

STÉPHANE BÉLAIR, ROSS BROWN, JOCELYN MAILHOT, AND BERNARD BILODEAU

Meteorological Research Branch, Meteorological Service of Canada, Dorval, Quebec, Canada

LOUIS-PHILIPPE CREVIER

Canadian Meteorological Centre, Meteorological Service of Canada, Dorval, Quebec, Canada

(Manuscript received 12 April 2002, in final form 15 October 2002)

ABSTRACT

The performance of a modified version of the snow scheme included in the Interactions between Surface–Biosphere–Atmosphere (ISBA) land surface scheme, which was operationally implemented into the regional weather forecast system at the Canadian Meteorological Centre, is examined in this study. Stand-alone verification tests conducted prior to the operational implementation showed that ISBA's new snow package was able to realistically reproduce the main characteristics of a snow cover, such as snow water equivalent and density, for five winter datasets taken at Col de Porte, France, and at Goose Bay, Newfoundland, Canada. A number of modifications to ISBA's snow model (i.e., new liquid water reservoir in the snowpack, new formulation of snow density, and melting effect of incident rainfall on the snowpack) were found to improve the numerical representation of snow characteristics.

Objective scores for the fully interactive preimplementation tests carried out with the Canadian regional weather forecast model indicated that ISBA's improved snow scheme only had a minor impact on the model's ability to predict atmospheric circulation. The objective scores revealed that only a thin atmospheric layer above snow-covered surfaces was influenced by the change of land surface scheme, and that over these regions the essential behavior of the atmospheric model was not significantly altered by improvements to the treatment of snow cover. It was shown that this lack of response was most likely related to the treatment of the snow cover fraction in each atmospheric model grid tile. The estimation of snow cover fraction relied on simple formulations that were dependent on poorly known parameters, such as the fractional coverage of vegetation. Results showed that uncertainties of only 15% in vegetation fractional coverage could be responsible for uncertainties of as much as 1–1.5 K in screen-level air temperature. This indicates that some care must be exercised in the specification of vegetation and snow cover fractional coverage.

1. Introduction

The importance for atmospheric models to correctly represent fluxes of heat, moisture, and momentum over snow-covered surfaces has long been recognized for short-, medium-, and long-range (i.e., seasonal and climate) simulations. Several investigators have demonstrated, for instance, the cooling effect in the atmosphere's lowest levels associated with the presence of snow, due to its high albedo and relatively low thermal conductivity (Namias 1985; Walsh et al. 1985; Ellis and Leathers 1999; Viterbo and Betts 1999). Others have described the role of snow in generating mesoscale ''snow breeze'' atmospheric circulations (Segal et al. 1999), as well as larger-scale circulations, such as monsoons (see Hahn and Shukla 1976; Barnett et al. 1989; Cohen and Rind 1991).

In an effort to improve the representation of this aspect of environmental modeling, a large number of snow models of varying degrees of complexity have been developed in the last decade or so. The common practice in atmospheric models was mainly, until a few years ago, to use very simple snow models in which the snow properties (thermal conductivity, heat capacity, albedo, density) were prescribed as a function of latitude and time of year (e.g., Manabe 1969; Marshall et al. 1994; Mailhot et al. 1997). Obviously, these simple formulations were not able to represent the evolution of the characteristics of snow and did not perform well in conditions that deviated from the prescribed snow cover climatology.

Snow packages of intermediate complexities are now more frequently used in atmospheric models (e.g., Verseghy 1991; Douville et al. 1995; Yang et al. 1997; Sun et al. 1999; Boone and Etchevers 2001). In these models,

Corresponding author address: Dr. Stéphane Bélair, Recherche en Prévision Numérique, 2121 Trans-Canada Highway, Room 500, Dorval, QC H9P 1J3, Canada.
E-mail: stephane.belair@ec.qc.ca

the characteristics of snow for a few snow layers (typically from 1 to 3) evolve in a prognostic manner. The complexity of these schemes is referred to as ''intermediate'' compared to ''detailed'' multilayer models (e.g., Anderson 1976; Brun et al. 1989; Jordan 1991; Loth et al. 1993) that resolve the vertical structure of snow temperature, density, and crystal structure.

It should be noted that in the above process of model evolution the emphasis was mainly placed on improving the representation of ''vertical'' processes, such as increasing the number of layers in the snowpack; using more computationally expensive diffusion equations; and better representing internal processes, such as water percolation and vapor transport. Other aspects, such as upscaling snow properties and specifying snow cover fraction, which are more ''horizontal'' in nature, have received less attention (see Yang et al. 1997).

To our knowledge, very few studies have examined the relative importance of these horizontal and vertical processes. For example, is it really necessary to use complex formulations of snow's vertical characteristics in the context of weather forecasting? Comparison studies have shown that simple snow models are able to reproduce the evolution of snow properties as well as more complex models (Jin et al. 1999; Essery et al. 1999). Moreover, the large uncertainties in critical surface characteristics, such as vegetation (e.g., height, leaf area index, fractional coverage), coupled with large uncertainties in atmospheric forcing (e.g., precipitation amount and phase, and downwelling radiation fluxes), have to be considered when assessing the need to increase the complexity of snow models.

The first objective of this study is, therefore, to evaluate to what degree a relatively simple snow scheme, with a single layer and with simple hydrology and thermal physics, is capable of adequately representing the main characteristics of snow, and to quantify the effect this snow scheme has on numerical weather prediction. The second aim of this study is to document the operational implementation of this simple snow scheme into the Canadian short-range regional weather forecasting system.

The snow model used is a modified version of the scheme originally introduced into the Interactions between Surface–Biosphere–Atmosphere (ISBA) land surface scheme (Noilhan and Planton 1989; Bélair et al. 2003) by Douville et al. (1995) (see section 2). The performance of this snow model is first evaluated in the context of ''stand alone'' experiments using data from Col de Porte, France, and Goose Bay, Newfoundland, Canada (see section 3). Finally, the impact of the new snow package on weather forecasting is examined using results from preimplementation parallel runs conducted in March 2001 with the Canadian regional operational model (see section 4).

2. ISBA snow package

The ISBA land surface scheme was developed in the late 1980s at Météo-France (Noilhan and Planton 1989).

TABLE 1. Modifications from Douville et al. (1995) snow scheme.

No.	Modification
1	New reservoir for liquid water retained in the snowpack (variable W_L) with exchanges (melt_s and freez_s with the snow mass reservoir (i.e., W_s).
2	Melting effect due to incident rainfall on the snowpack.
3	More sophisticated representation of the snow density, i.e., diagnostic calculations for the max snow density and for the density of fresh snow, and the effect of freezing on the snow density.

This scheme is the central component of the new surface modeling system that was operationally implemented in September 2001 at the Canadian Meteorological Centre (CMC). The details of this implementation, as well as a description of CMC's version of ISBA (except for the cold climate aspects of the surface scheme) are given in Bélair et al. (2003).

The snow package in CMC's implementation of ISBA was originally developed by Douville et al. (1995). This package was significantly modified to address a number of over simplifications, which are discussed later in section 3. These modifications are listed in Table 1, and are described, together with other aspects of ISBA's snow model, in the rest of this section.

a. Thermal properties of the surface

The force–restore equations for ISBA's surface temperatures T_S and T_2 and the calculations for the surface thermal coefficient are given in Eqs. (1)–(5) of Bélair et al. (2003). (Descriptions of ISBA's most important variables, including all the prognostic variables, are given in Tables 2 and 3 of the same paper.) One of ISBA's main features is that only one energy budget is performed over the land portion of a model grid area. The surface thermal coefficient thus includes the effect of bare soil, vegetation, and snow, which are weighted by the fraction of the model grid area covered by vegetation (veg) and snow (p_{sn}), and the fraction of bare soil and vegetation covered by snow (p_{sng} and p_{snv}). The snow-covered fractional grid areas, following Blondin (1989) and Pitman et al. (1991), are given by

$$p_{\text{sng}} = \frac{W_S}{W_{\text{crn}}}, \qquad p_{\text{sng}} \leq 1; \tag{1}$$

$$p_{\text{snv}} = \frac{h_S}{(h_S + 5z_0)}; \tag{2}$$

$$p_{\text{sn}} = (1 - \text{veg})p_{\text{sng}} + \text{veg}p_{\text{snv}}; \tag{3}$$

in which W_S is the snow mass (not including the liquid water retained in the snow layer), $W_{\text{cm}} = 10$ kg m^{-2}, $h_S = W_S/\rho_{\text{snow}}$ is the snow depth (m), ρ_{snow} is the density of snow, and z_0 is the surface roughness length. For example, a 50-cm snowpack (equivalent to $W_S = 50$ kg m^{-2}) with a density $\rho_{\text{snow}} = 100$ kg m^{-3} will lead to $p_{\text{sng}} = 1.0$, and $p_{\text{snv}} \sim 0.10$ for $z_0 = 1$ m (e.g., tall

forests) or $p_{snv} \sim 0.90$ for $z_0 = 0.01$ m (e.g., grass). The total snow cover fraction p_{sn} would then be about 0.33 for forests and 0.92 for grass for grid areas covered 80% by vegetation (i.e., veg = 0.80).

The thermal coefficient for snow is given by

$$C_S = 2\left(\frac{\pi}{\lambda_S c_S \tau}\right)^{1/2}, \tag{4}$$

where $\lambda_S = \lambda_i \rho_S^{1.88}$ is the snow thermal conductivity (Yen 1981) and $c_S = c_i(\rho_S/\rho_i)$ is the heat capacity of snow in which $\rho_S = \rho_{snow}/\rho_{water}$ is the relative density of snow; ρ_{water} is the density of water; and λ_i, c_i, and ρ_i are the thermal conductivity, heat capacity, and relative density of ice, respectively.

b. ISBA's water budget

The water budget represented in CMC's implementation of ISBA is shown schematically in Fig. 1 of Bélair et al. (2003). The details of the prognostic equations for soil volumetric water contents w_g and w_2 and the expressions for surface fluxes are also given in this paper. Here, we will discuss the representation of the prognostic variables related to snow, that is, the snow mass W_S, liquid water W_L retained in the snowpack, relative snow density ρ_S, and snow albedo α_S. ISBA does not have, at this time, a specific reservoir (prognostic variable) for snow intercepted by the vegetation canopy.

It can also be noted from the water budget diagram that this version of ISBA includes an additional prognostic variable for frozen soil water. This aspect of surface modeling has been shown to have some influence, in certain conditions, on the evolution of the snowpack (Slater et al. 1998; Schlosser et al. 2000). However, sensitivity studies with ISBA's relatively simple formulation of snow processes only revealed a weak impact of soil freezing/thawing on snow's properties. It was therefore decided, for the sake of clarity and conciseness, to delay discussion of ISBA's frozen soil aspect (variable w_f and conversion terms freez_g and melt_g) to subsequent publications.

c. Snow mass

The evolution of the snow mass W_S is given by

$$\frac{\partial W_S}{\partial t} = P_S - E_S + \text{freez}_S - \text{melt}_S, \tag{5}$$

where P_S is the snowfall rate and E_S is the sublimation rate of snow. The snow freezing and melting exchanges between the W_S and W_L reservoirs are represented in this way:

$$\text{freez}_S = \frac{p_{sn}(T_0 - T_n)}{C_S L_f \Delta t} \quad \text{and}$$

$$0 \le \text{freez}_S \le \frac{W_L}{\Delta t}, \tag{6}$$

$$\text{melt}_S = \frac{p_{sn}(T_n - T_0)}{C_s L_f \Delta t} + \text{melt}_{rain} \quad \text{and}$$

$$0 \le \text{melt}_S \le \frac{W_S}{\Delta t}, \tag{7}$$

in which $T_n = (1 - \text{veg})\, T_S + \text{veg}\, T_2$ is, in the context of a single energy budget land surface scheme, a snow surface temperature that is a combination of T_S (for snow over bare soil) and T_2 (for snow under the vegetation canopy); $T_0 = 273.16$ K is the melting/freezing temperature; melt_{rain} is for snow melting associated with rainfall; and Δt is the model time step.

d. Melting effect of rainfall incident on the snowpack

The melting term melt_{rain} in (7) accounts for modification of snow's internal energy due to incident liquid precipitation that is warmer than T_0. By using the concept of enthalpy conservation (which reduces here to internal energy conservation $h = c_p T$), it can be shown that the surface temperature of snow is increased by ΔT_{snow} in the case of incident rainfall:

$$\Delta T_{snow} = \frac{P_r \Delta t (T_{rain} - T_{snow})}{(W'_S + W'_L) + P_r \Delta t} \tag{8}$$

in which $W'_S + W'_L$ is the total amount of water in the snowpack that is involved in the energy transfer between the incident liquid precipitation and the snowpack. The quantity $(P_r \Delta t)$ is the liquid water reaching the surface during a single time step (kg m^{-2}), and T_{rain} is the temperature of rain falling on the snowpack (taken, for the moment, equal to the low-level air temperature).

It is important to note that snow's surface temperature T_{snow} is used in (8) instead of the surface temperature T_S. Unfortunately, T_{snow} is not predicted in ISBA's current version, in which the energy budget over snow is merged with the snow-free portion of the model grid area. To get around this problem, the surface temperature of snow is presumed to be equal to T_0 (i.e., the melting/freezing temperature), which seems a reasonable assumption considering that low-level atmosphere is warm enough to produce rain. If we also presume that $W'_S + W'_L = (P_r \Delta t)$, then (8) simply becomes

$$\Delta T_{snow} = \frac{T_{rain} - T_0}{2}, \tag{9}$$

and the melting rate due to incident liquid precipitation can be calculated using

$$\text{melt}_{rain} = \frac{T_{rain} - T_0}{2 C_S L_f \Delta t}, \qquad \text{melt}_{rain} \ge 0. \tag{10}$$

e. Liquid water in the snowpack

The liquid water W_L retained in the snow layer evolves according to

$$\frac{\partial W_L}{\partial t} = p_{\text{sn}}(P_r + R_{\text{veg}}) - R_{\text{snow}} + \text{melt}_S - \text{freez}_S. \quad (11)$$

When the amount of liquid water in the snow approaches and exceeds a critical value W_{Lmax}, there is snowmelt runoff, following Loth et al. (1993):

$$R_{\text{snow}} = \frac{W_{\text{Lmax}}}{\tau_{\text{hour}}} \exp[W_L - W_{\text{Lmax}}] \quad \text{if } W_L \le W_{\text{Lmax}}, \quad (12)$$

$$R_{\text{snow}} = \frac{W_{\text{Lmax}}}{\tau_{\text{hour}}} + \frac{W_L - W_{\text{Lmax}}}{\Delta t} \quad \text{if } W_L > W_{\text{Lmax}}, \quad (13)$$

where

$$W_{\text{Lmax}} = c^R W_S; \quad (14)$$

τ_{hour} is a 1-h time constant, and c^R is a retention factor that depends on the density of the snow, following

$$c^R = c^R_{\text{min}} \quad \text{if } \rho_S \ge \epsilon_e, \quad (15)$$

$$c^R = c^R_{\text{min}} + (c^R_{\text{max}} - c^R_{\text{min}})\frac{\rho_e - \rho_S}{\rho_e} \quad \text{if } \rho_S < \rho_e, \quad (16)$$

with $c^R_{\text{min}} = 0.03$, $c^R_{\text{max}} = 0.10$, and $\rho_e = 0.2$.

f. Snow albedo

The evolution of snow albedo α_S is based on Verseghy (1991). In this formulation, snow albedo decreases linearly or exponentially with time, depending if snow is melting or not:

$$\alpha_S(t) = \alpha_S(t - \Delta t) - \tau_a\frac{\Delta t}{\tau} + \frac{P_S\Delta t}{W_{\text{cm}}}(\alpha_{\text{Smax}} - \alpha_{\text{Smin}}) \quad (17)$$

for cold snow (i.e., without melting), and

$$\alpha_S(t) = \alpha_{\text{Smin}} + [\alpha_S(t - \Delta t) - \alpha_{\text{Smin}}] \exp\left[-\tau_f\frac{\Delta t}{\tau}\right] \quad (18)$$

for warm snow (i.e., with melting). Here $\tau_a = 0.008$, $\alpha_{\text{Smin}} = 0.50$, $\alpha_{\text{Smax}} = 0.80$, and $\tau_f = 0.24$.

g. Snow density

The relative snow density ρ_S evolves according to an extension of the formulation described in Verseghy (1991). In this new formulation, snow density first increases due to gravitational settling, following the exponential function:

$$\rho'_S = \rho_{\text{Smax}} - [\rho_{\text{Smax}} - \rho_S(t - \Delta t)] \exp\left(-\tau_f\frac{\Delta t}{\tau}\right) \quad \text{if } \rho_S(t - \Delta t) < \rho_{\text{Smax}}, \quad (19)$$

$$\rho'_S = \rho_S(t - \Delta t) \quad \text{if } \rho_S(t - \Delta t) \ge \rho_{\text{Smax}}, \quad (20)$$

in which ρ_{Smax} is the maximum snow relative density given as a function of snow depth, following Tabler et al. (1990):

$$\rho_{\text{Smax}} = \frac{1}{\rho_{\text{water}}}\left\{600 - \frac{20.47}{h_S}\left[1 - \exp\left(-\frac{h_S}{0.0673}\right)\right]\right\} \quad \text{if } \text{melt}_S > 0, \quad (21)$$

$$\rho_{\text{Smax}} = \frac{1}{\rho_{\text{water}}}\left\{450 - \frac{20.47}{h_S}\left[1 - \exp\left(-\frac{h_S}{0.0673}\right)\right]\right\} \quad \text{if } \text{melt}_S = 0. \quad (22)$$

The intermediate value of snow density (ρ'_S) is used as the starting point for the second mechanism according to which snow density decreases due to fresh snow:

$$\rho''_S = \frac{(W^i_S - P_S\Delta t)\rho'_S + P_S\Delta t\rho_{\text{Snew}}}{W^i_S}, \quad (23)$$

where $W^i_S = \max(W_S, P_S\,\Delta t)$ and ρ_{Snew} is the relative density of fresh snow, which is calculated following the formulation used in the more sophisticated CROCUS snow model (see Brun et al. 1989):

$$\rho_{\text{Snew}} = \frac{1}{\rho_{\text{water}}}[109 + 6(T_a - T_0) + 26V_a^{1/2}] \quad (24)$$

with

$$0.100 \le \rho_{\text{Snew}} \le 0.250,$$

in which T_a and V_a are temperature and wind speed at 1.5- and 10-m above ground, respectively. Finally, the change of snow density due to freezing of liquid water is considered, following

$$\rho_S(t) = \left(\frac{W_S}{W_S + \text{freez}_S\Delta t}\right)\rho''_S + \left(\frac{\text{freez}_S\Delta t}{W_S + \text{freez}_S\Delta t}\right)\rho_i, \quad (25)$$

in which $\rho_i = 0.9$ is the relative density of ice. Because of (25), snow density can be larger than ρ_{Smax}, which sometimes occurs near the end of the cold season.

3. Stand-alone experiments

a. Observational datasets

Before investigating the impact of the improved snow package on wintertime short-range weather forecasting, its performance was evaluated in stand-alone mode at

TABLE 2. Observational data for the stand-alone experiments.

Name	Acronym	Lat/lon (°)	Elevation (m)	Mean air pressure (hPa)	Season
Col de Porte (France)	CdP	45.30°N 5.77°E	1340	840	10 Oct 1993–10 Apr 1994 20 Dec 1994–20 Apr 1995
Goose Bay (Canada)	GB	53.32°N 60.42°W	46	1005	1 Sep 1969–30 Jun 1970 1 Sep 1971–30 Jun 1972 1 Sep 1972–30 Jun 1973

two sites: Col de Porte (hereafter CdP) in the Fench Alps, and Goose Bay (hereafter GB) in Newfoundland, Canada. In stand-alone mode, observed atmospheric conditions (i.e., low-level air temperature and humidity, low-level wind speed, downwelling solar and infrared radiation at the surface, and precipitation) are directly used to derive the snow model.

Data from CdP have been used extensively in snow model validation and development (see Brun et al. 1989; Douville et al. 1995; Essery et al. 1999; Boone and Etchevers 2001), and both CdP and GB datasets are currently being used in the Snow Model Intercomparison Project (SnowMIP) experiment (Essery et al. 1999). The two sites represent contrasting snow-climate regions: temperate–alpine for CdP, with high precipitation but relatively mild temperatures; and maritime–boreal for GB–with much colder temperatures and larger wind speeds. As indicated in Table 2, the CdP observation site was located at a relatively high altitude (1340 m) on relatively flat terrain that was well protected from wind by dense and high coniferous forests. Soil was covered by short grass and was not frozen, in general. Observations taken during 1993/94 and 1994/95 winters are used in this study and included snow water equivalent (SWE) and snow density, as well as surface temperature and snowmelt runoff.

The GB observation site was quite different. It was located at a much lower altitude (46 m), and observations were taken in an unprotected open area. Vegetation around the GB site was sparse black spruce and the soil was covered by lichen. Also, the low temperatures that are generally observed in this region of Canada could lead to much different characteristics of snow as compared to CdP, which is not as cold. The first 10–20 cm of the soil are typically frozen during winter, but there was no permafrost layer at this site. Hourly forcing data are available at the GB site for a period of 15 yr (from 1969 to 1984). In the present study, only data for the 1969/70, 1971/72, and 1972/73 winters are examined. It must be mentioned that the incoming longwave fluxes were not measured at GB, so values were estimated using air temperature, relative humidity, cloud type, and cloud opacity [following Idso (1981) and Sellers (1965)]. Snow depth, density, and SWE were measured at GB but there were no observations of snow surface temperature or snowmelt runoff.

b. Characteristics of the snowpack

The two versions of ISBA's snow package discussed in this study, that is, the one described in Douville et al. (1995) (referred to as the ''original'' or ''old'' version) and the one described in section 2 (referred to as the ''new'' or ''modified'' version), as well as the CROCUS snow model, were all tested against the CdP and GB datasets.

As mentioned in the previous section, ISBA's original snow package is similar to the new snow scheme (see Douville et al. 1995), except for the liquid water reservoir in the snowpack, the melting effect of incident rainfall, and the new formulation of snow density. The CROCUS snow model, on the other hand, is a much more sophisticated energy and mass model that was developed for operational avalanche forecasting (see Brun et al. 1989, 1992). In this model, up to 50 snow layers are used to represent internal snow processes and variations in properties through the depth of the snow. Comparative descriptions of CROCUS and ISBA original formulation (as well as two other snow schemes) are given in Essery et al. (1999).

Comparisons of observed and simulated snow characteristics (i.e., SWE, snow depth, and snow density) for these three models are shown in Figs. 1–5. These figures clearly show the improvement resulting from the modifications to ISBA's snow package. The most obvious improvement is the representation of snow density. In the original formulation, density rapidly increases toward an asymptotic value of 300 kg m^{-3} which does not compare well with the observations. This is particularly true for CdP data, which shows snow density reaching values higher than 300 kg m^{-3} very quickly during the first months of winter. The modified version of ISBA's snow model provides a realistic simulation of snow density for all the years of data tested in this study, except maybe for the 1969/70 winter at GB, when the density remained more or less constant for most of winter.

The simulation of SWE is also much improved by the modifications in ISBA's snow package (see Figs. 1–5). The original version greatly underestimates spring melt and has snow on the ground for several weeks longer than what is observed (e.g., see Fig. 3). This problem is practically eliminated with the modified

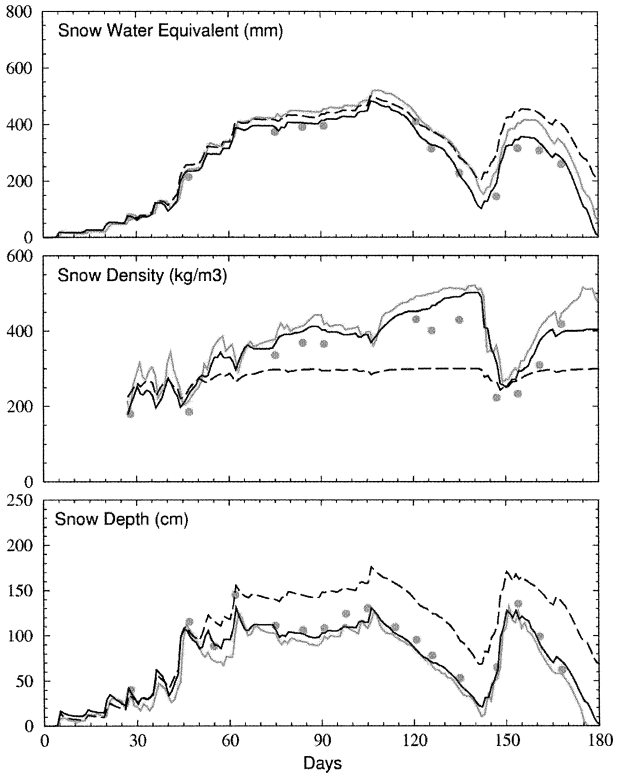

FIG. 1. Comparison between simulated and observed snow characteristics for winter 1993/94 at Col de Porte, France. Results from modified and original ISBA snow models (full and dashed black lines, respectively) and CROCUS (full gray lines) are shown. The large gray dots represent observations.

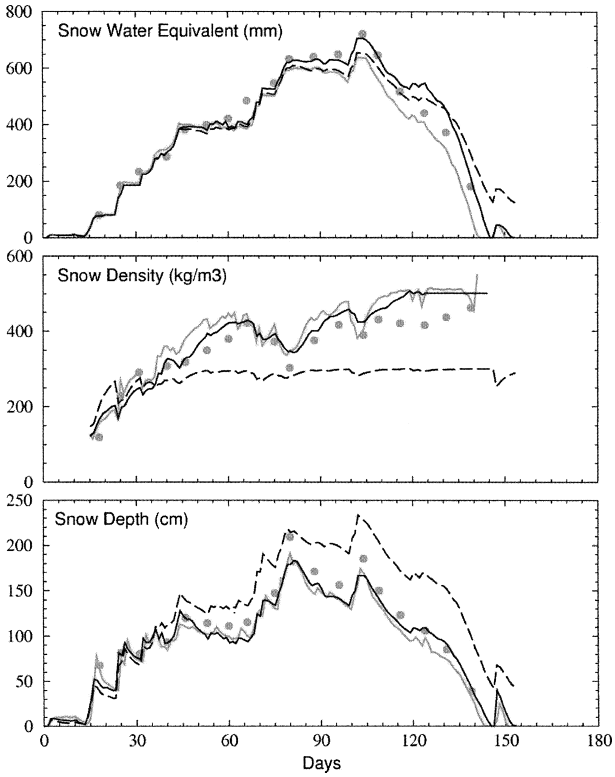

FIG. 2. Same as Fig. 1, but for winter 1994/95.

snow model, which is able to closely reproduce the evolution of SWE for all the years simulated in this study.

The poor representation of SWE and snow density by the original package lead to even greater errors for snow depth, which is often too large compared with observations. For CdP, these errors on snow depth can be as large as 30–40 cm (see Figs. 1 and 2). For GB, the overestimation of snow depth is mainly found during the last (melting) portion of winter. The problem is not as serious at GB during the rest of the cold season because snow density at this site remains close to 300 kg m^{-3} during much of the winter. This overestimation is not observed with the modified version of the snow package, which represents the evolution of snow depth in a very acceptable manner.

The results obtained with the new version of ISBA's snow package are comparable to CROCUS (see Figs. 1–5), except for the 1969/70 and 1972/73 winters at GB, where CROCUS better represented the snow density during the middle portion of the cold season (especially around days 160–180 in 1969/70 when CROCUS captured an event that ISBA did not). This positive performance of ISBA's modified snow package is encouraging, considering the relative simplicity of this scheme compared to CROCUS. The results obtained

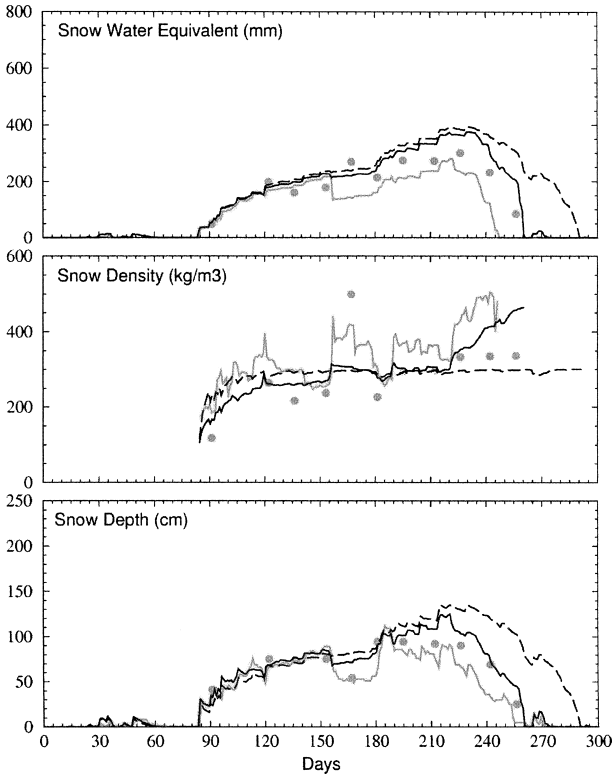

FIG. 3. Same as Fig. 1, but for winter 1969/70 at Goose Bay, Newfoundland, Canada.

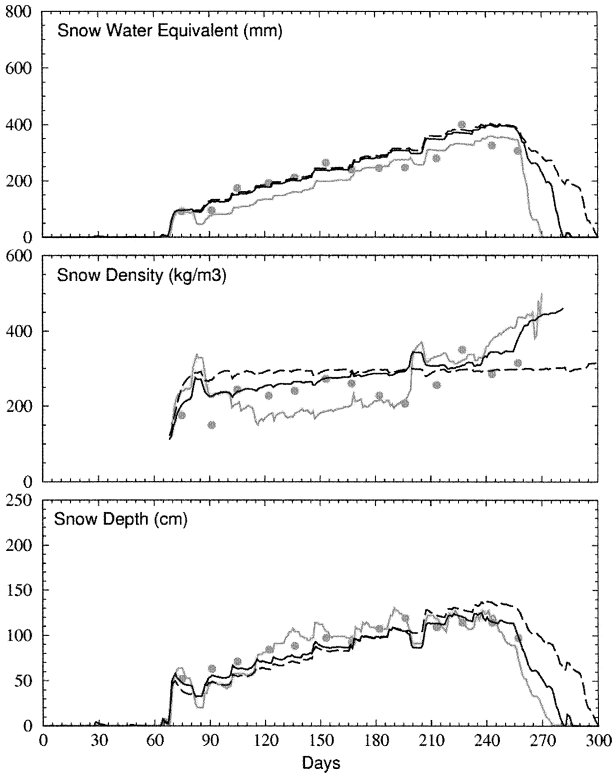

FIG. 4. Same as Fig. 1, but for winter 1971/72 at Goose Bay, Newfoundland, Canada.

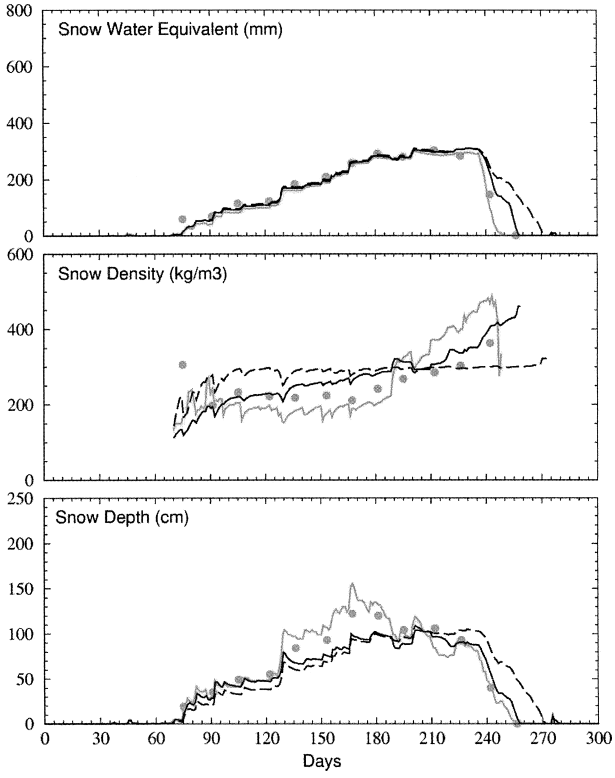

FIG. 5. Same as Fig. 1, but for winter 1972/73 at Goose Bay, Newfoundland, Canada.

with this scheme for CdP's two winter seasons (1993/94 and 1994/95) also compare favorably with other schemes of similar or greater complexity (Sun et al. 1999; Essery et al. 1999; Boone and Etchevers 2001).

To understand the reasons for these good results in the stand-alone mode, the CdP 1993/94 winter season was used as a test case for systematically examining the impact of each snow modification (see Table 1). In these simulations, the original formulation of snow density was used (experiment ORIDEN), the new reservoir for liquid water retained in the snowpack was removed (experiment NOWL), and the melting effect of incident rainfall was not considered (experiment NORAIN). Results are shown in Fig. 6.

When using the original formulation of the snow density, the asymptotic behavior of this variable is reproduced, with values tending toward 300 kg m^{-3} (see experiment ORIDEN in Fig. 6). Because this value is smaller than the observed snow density (typically around 400 kg m^{-3}), the snow depth is significantly overestimated for this sensitivity experiment (by at least a few tens of centimeters). It is interesting to note that this change in snow density is also responsible for a different evolution of SWE during the second half of the cold season. Because of the smaller heat capacity and thermal conductivity associated with smaller values of snow density, melting between days 120 and 140 is significantly underestimated when using the original formulation of the snow density [see Eqs. (4) and (7)]. This weaker melting is responsible for extending the snow-covered period by about 2 weeks for this dataset.

It is evident from Fig. 6 that inclusion of the liquid water reservoir in the snow layer also improves the snowpack simulation. Without this new reservoir, liquid water resulting from snow melting goes directly to the soil, without any transition period associated with percolation and retention within the snowpack. The most obvious consequence of this lack of retention is that SWE decreases too rapidly during melting periods; this leads to an early end of the snow-covered season, by a few days compared to observations, for the 1993/94 winter season at CdP. When percolating snowmelt is immediately drained from the snowpack without a retention factor, as it is in the case of experiment NOWL, the increase of snow density due to refreezing effects is not possible. This is why the snow density for this sensitivity experiment is reduced when the liquid water reservoir is omitted. In this particular case, the snow density obtained in experiment NOWL agrees better with observations. This may indicate that the increase of density due to refreezing processes could be overestimated in the new version of ISBA's snow package.

Finally, the numerical representation of melting effects associated with the rainfall events that occurred during 1993/94 CdP winter also appear to have improved the simulation of the characteristics of snow (see

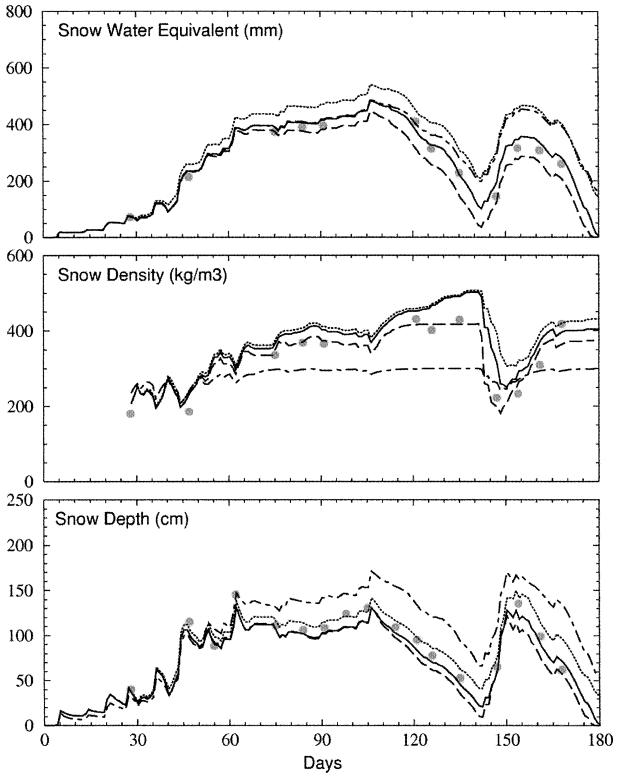

FIG. 6. Sensitivity experiments for the simulation of winter 1993/94 Col de Porte data. Results with the full new version of ISBA's snow model are shown by the full lines. Simulations with no liquid water in the snow pack (experiment NOWL; dashed lines), with no melting effect caused by incident rainfall (experiment NORAIN; dotted lines), and with the original formulation of snow density (experiment ORIDEN; dash–dotted lines) are also plotted. The large gray dots represent observations.

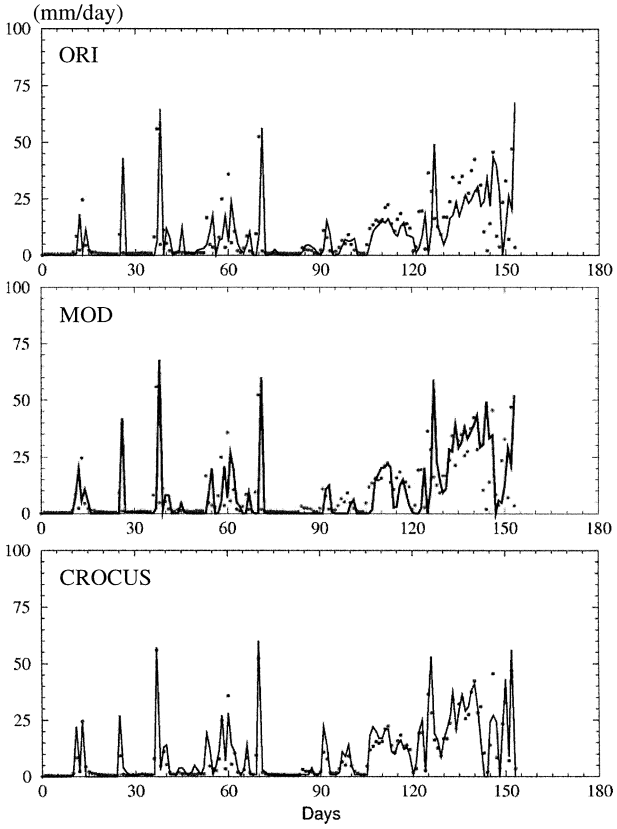

FIG. 7. Simulated (full lines) snowmelt runoff (mm day^{-1}) for winter 1994/95 at Col de Porte. Results from the original and modified versions of ISBA's snow model, as well as for CROCUS, are shown. Observations are represented by the gray dots.

experiment NORAIN in Fig. 6). Without this melting effect, SWE and snow depth remain larger than observations for most of the CdP 1993/94 winter season. The end of the snow-covered period is thus delayed by about 2 weeks for this sensitivity experiment. Furthermore, the representation of snow density is slightly deteriorated when this effect is not considered.

c. Snowmelt runoff

Snowmelt runoff can also be examined in order to evaluate the performance of ISBA's new snow package. Correct representation of this quantity is of obvious importance for driving hydrological models (e.g., Aguado 1985; Garen et al. 1999). Figures 7 and 8 compare observed and simulated daily and cumulative snowmelt runoff for CdP in the winter of 1994/95. Except for a few minor differences, Fig. 7 shows that all three snow models are able to represent, in an acceptable manner, daily snowmelt runoff under the snowpack, at least for this particular case.

Some differences between snowmelt runoff from the three snow schemes can be seen in Fig. 8. For the first half of the CdP 1994/95 winter, that is, up to day 110, the total snowmelt runoff accumulation is best represented by ISBA's original snow package. Up to this day, the modified snow package underestimates the snowmelt runoff, whereas CROCUS overestimates it. For the second half of the cold season, ISBA's original snow model underestimates the snowmelt runoff, and vice

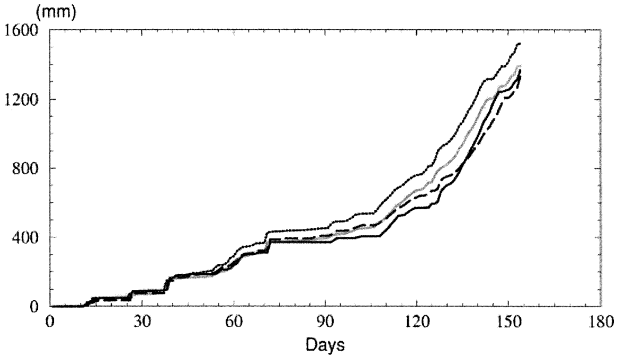

FIG. 8. Accumulated snowmelt runoff (mm) for winter 1994/95 at Col de Porte. Results from ISBA's original and new snow package are shown (dashed and full lines), as well as results from CROCUS (dotted line) and observations (full gray line).

versa, for the modified version of the snow scheme. The final result is that the total snowmelt runoff accumulations at the end of winter are quite close to observation (~1400 mm) for the two ISBA snow schemes, while total snowmelt runoff accumulation from CROCUS is slightly too large (~1500 mm).

The snowmelt runoff results shown in this study are comparable to those presented in Essery et al. (1999) for the same dataset. Our results do not seem, however, to be as good as those described in Boone and Etchevers (2001) who used a three-layer snow model for the same winter simulation. This difference between the two studies may indicate that numerical representation of snowmelt runoff could be sensitive to the parameterization of physical processes in the snowpack, especially near the soil–snow interface. For instance, melt/refreeze processes within the snowpack are not handled well in single-layer snow models. Nevertheless, it seems clear that the physical processes included in the modified ISBA's snow model have a lesser impact on snowmelt runoff than they have on the simulation of snow density and SWE, at least for the CdP data. Because snowmelt runoff mainly depends on atmospheric forcing (radiation, air temperature, and low-level wind), it appears that a simple formulation of physical processes (such as that in the original version of ISBA's snow scheme) is sufficient to produce realistic values for this quantity.

d. Snow surface temperature

Snow surface temperature is very important for surface schemes used in atmospheric models, because this variable plays a major role in the determination of exchanges of heat and moisture between the snow surface and the atmosphere. Figure 9 shows a statistical comparison between simulations and observations of snow surface temperatures for the 2 yr of CdP data. Erroneous surface temperature observations identified by Essery et al. (1999) and Bonne and Etchevers (2001) were omitted for this comparison.

The results shown in Fig. 9 indicate that the modifications to ISBA's snow package did not improve the simulation of snow surface temperature. It is true that statistical computations reveal that the small bias from ISBA's original version is mainly eliminated with the new scheme (from −0.51 to −0.09 K), and that this new bias even compares favorably against that of CROCUS (−0.62 K). But this improvement is of secondary importance, in our opinion, compared to the fact that the root-mean-square (rms) errors for the two ISBA versions remain almost identical (i.e., 2.0 and 2.1 K), which is approximately twice as large as the rms error calculated for CROCUS (i.e., 1.1 K). This larger rms error can be clearly seen in Fig. 9.

The difference in rms error between the two models is mainly due to the fact that snow is treated as a single layer in ISBA, where the surface temperature evolves according to a force–restore equation in which a ''di-

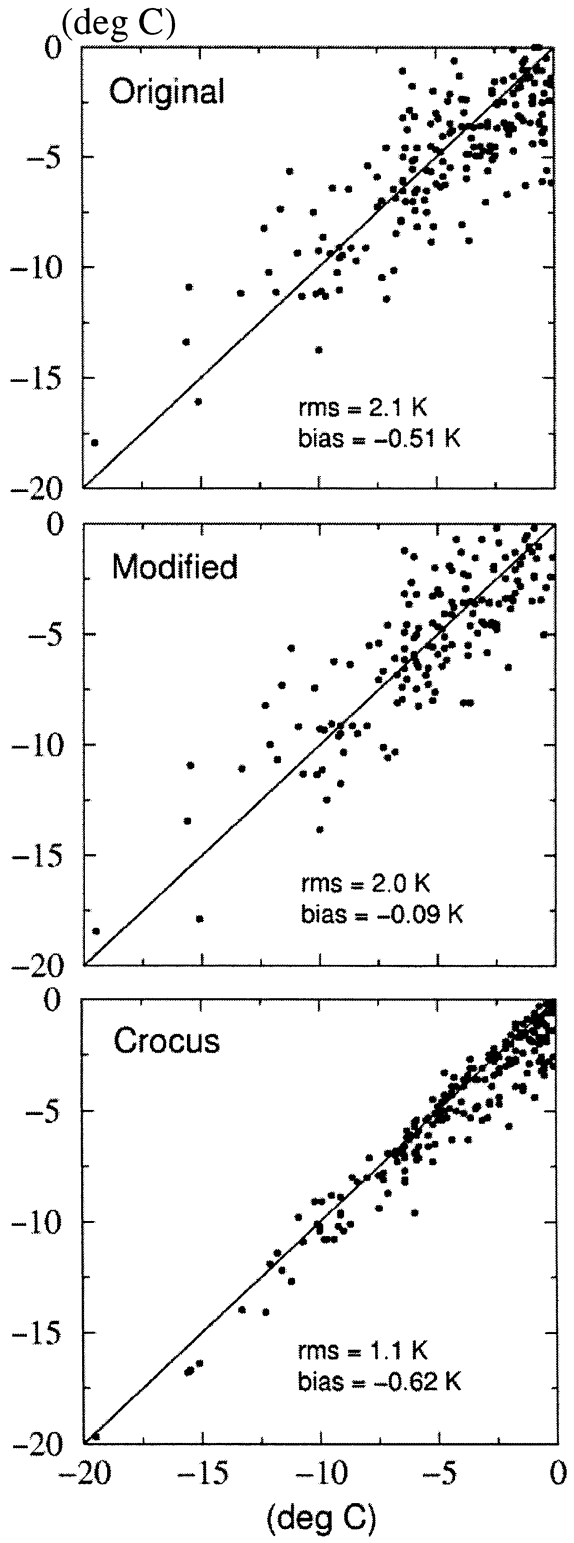

FIG. 9. Scatterplots of observed and simulated snow surface temperature (°C) for the two winters of Col de Porte data. The rms errors and biases are also given.

urnal'' diffusion is parameterized [see (2) and (3) of Bélair et al. (2003)]. In CROCUS, a large number of layers are used (~50), combined with a surface energy budget and a heat diffusion equation for determining the snow temperature at the surface and in the rest of the snowpack. For this reason, CROCUS is able to capture vertical profiles of density and temperature that a single-layer snow model is unable to do.

Even though a few investigators have argued in the past that the force–restore technique may lead to a better representation of snow surface temperature, compared to bulk-layer diffusive/iterative energy models (see Yang et al. 1997; Slater et al. 2001), we believe that the differences observed between ISBA's snow schemes and CROCUS are due to a better representation of the temperature profile in the snowpack, especially in the layers near the surface. Results presented in Boone and Etchevers (2001) may confirm this hypothesis because they have noted, for the same CdP dataset, a reduction of rms error for snow surface temperature (from 2.34 to 1.85 K; see their Table 2) associated with the use of a three-layer model, compared to a force–restore type model similar to the one used in the present study. Of course, other factors could explain this improvement. However, their results, together with the potential for better representing other snow processes like snow melting and runoff, encourages us to adopt a similar strategy (with maybe more than three layers) in the future.

4. Preimplementation tests: Impact on atmospheric weather forecasting

a. Objective evaluation

The modified version of ISBA's snow package was operationally implemented at CMC in September 2001, as part of the new surface modeling system described in Bélair et al. (2003). Prior to this implementation, numerous tests were done to evaluate the impact of this new surface modeling system on numerical weather forecasting, which is the principal interest of CMC. The incorporation of ISBA during the warm season gave very positive results (Bélair et al. 2003). However, as explained in the rest of this section, the results were not as encouraging for cold season forecasting.

The cold season evaluation of the modified version of the land surface scheme was carried out by objectively scoring a series of 48-h forecasts initialized with analyses produced by a continuous assimilation cycle that covered the period from early January to the end of March 2001. Because a few of the surface prognostic variables required many weeks to spin up from approximative initial conditions, only results for March 2001 were examined in this study. Indeed, as is the case for snow-free surface variables (e.g., soil moisture; see Bélair et al. 2003), initial conditions for some of snow's prognostic variables are difficult to specify due to a lack of observations. This is the case for the liquid water retained in the snow layer, as well as snow albedo and density. In the continuous surface assimilation cycle that was performed, these three snow variables were carried on or transported from one 24-h integration to another; that is, results from 24-h integrations were used as initial conditions for the next-day forecast. The other snow variable, that is, snow mass, was reinitialized for every integration using an external snow depth analysis (see Brasnett 1999).

Results obtained from this series of integrations were compared against outputs from the regional model that was operational at the time at CMC. The surface scheme that was used operationally in this previous version of CMC's regional model is also based on the force–restore technique, but with much simpler treatments of vegetation and snow compared to ISBA (see Mailhot et al. 1997, 1998). In this less sophisticated scheme, the surface is considered as completely snow covered if snow depth is larger than or equal to 5 cm. In contrast with ISBA, only one type of surface is treated for each model grid tile, that is, bare ground, snow, or ice. In order to include effects resulting from the state of the snow (wet versus dry, old versus fresh), the snow's thermal conductivity and heat capacity are empirically determined from latitude and time of year. The vegetation impact on the surface temperature is obtained by modulating the heat capacity using the surface albedo. Large values of surface albedo indicate that the surface is mostly covered by snow and, thus, that vegetation has little effect on surface temperature (and vice versa for low values of albedo). This albedo is also useful in warm periods to partition the surface available energy between snow melting and vegetation canopy warming. In this highly parameterized surface scheme, the snow mass and snow albedo are kept constant during the atmospheric model integration. The initial snow mass is also given by the snow analysis described in Brasnett (1999).

The objective verification of screen-level air temperature and dewpoint depression (i.e., $T - T_d$, in which T_d is the dewpoint temperature) for the northern half of North America, which was mostly covered by snow during March 2001, revealed that using the modified version of ISBA did not significantly improve the numerical prediction of near-surface temperature and humidity during wintertime (see Fig. 10). In fact, it can be noted from the objective scores that rms and bias errors for temperature are larger with the new system. For dewpoint depression, the new system's errors are smaller compared to the previous operational model, but the improvement is not substantial.

The upper-air objective evaluation for the same time period and verification region, shown in Fig. 11, reveal that results from the two regional model configurations differ only for a thin atmospheric layer above the surface. The results from the two models are almost identical at 850 hPa and do not differ much at 925 hPa. This weak impact on the boundary layer numerical representation, of implementing a new, more physical, sur-

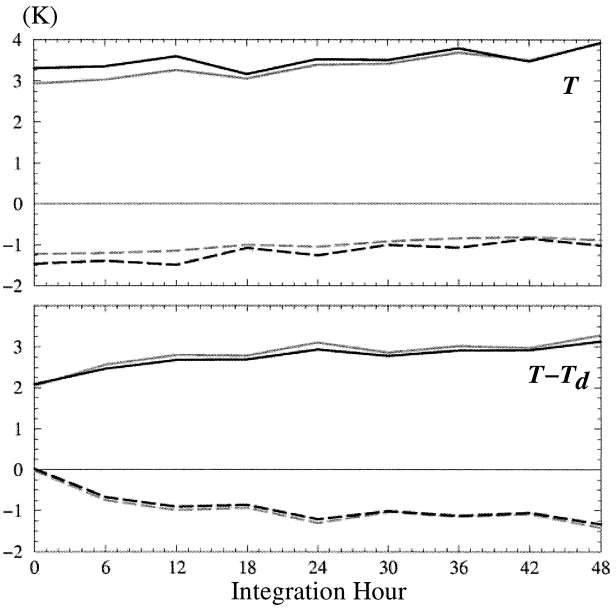

FIG. 10. Objective evaluation of (top) model screen-level temperature and (bottom) dewpoint depression ($T - T_d$) against observations for all the 0000 and 1200 UTC integrations conducted in Mar 2001. The rms errors are represented by the full lines whereas bias errors are shown by dashed lines. Scores for the operational and ISBA versions of the model are indicated by the gray and black lines, respectively.

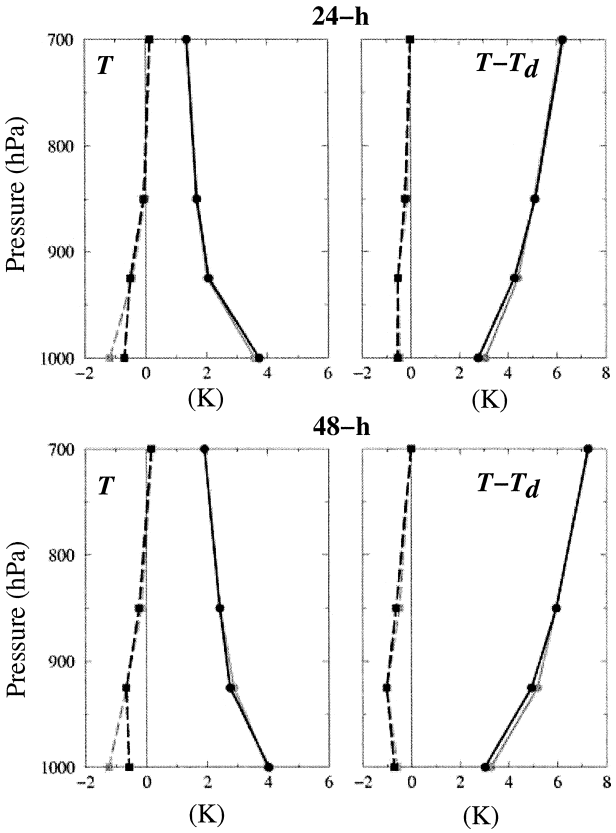

FIG. 11. Objective evaluation of upper-air temperature (T) and dewpoint depression ($T - T_d$) for Mar 2001 cases. Rms (K; full lines and circles) and bias (K; dashed lines and squares) errors are shown for 24- and 48-h integrations from the operational (gray lines) and ISBA (black lines) cycles.

face scheme could be explained by the relatively weak coupling that exists between the surface and the boundary layer in wintertime (due to small surface fluxes). Obviously, surface fluxes in wintertime do not generate as much turbulence as in summertime, and thus the boundary layer does not grow as high.

The verification at 1000 hPa reveals that the temperature rms errors at this level are slightly larger with the new surface scheme, whereas the cold bias at the same level is cut by half. For dewpoint depression, the rms errors are slightly smaller with ISBA at 1000 and 925 hPa, whereas the biases are very similar for the two model configurations. The apparent contradiction between the bias scores obtained from the surface stations and those calculated from 1000-hPa radiosonde data (cf. Figs. 10 and 11) could be explained by the fact that objective verification against 1000-hPa radiosonde data is probably not as meaningful as the surface evaluation (Fig. 10), due to issues such as interpolation (for radiosonde data), which may not capture the sharp temperature gradients that often exist near the surface in wintertime; and also because the number of verification couplets are significantly smaller at this 1000-hPa level which is, for many observation points, located below the surface.

Considering that precipitation scores for March 2001 are practically identical for the two model versions (not shown), it seems clear that adding more sophistication to the representation of snow in the Canadian regional forecasting model did not significantly improve wintertime weather forecasting, at least during this month of verification. This result was surprising, considering the ability that ISBA's modified snow package showed in representing the observed characteristics of snow for the CdP and GB stand-alone experiments. These positive stand-alone results were expected to translate into a much improved forecast of wintertime boundary layers (in a fully interactive mode), even though the two modeling systems were initialized with the same snow depth analysis. In the next subsection, possible reasons that could help understand this lack of improvement are discussed.

b. Discussion on the snow cover fraction

The lack of improvement related to the inclusion of ISBA's new snow package into the Canadian regional weather forecast model can be explained, in part, by the weak coupling that exists between the surface and the boundary layer in winter, and by the fact that the same snow mass fields were used to initialize both the control and ISBA runs. (Future studies are now being planned to investigate the meteorological impact of using results from the ISBA model as a first guess for the snow depth

assimilation.) Another factor is ISBA's limited ability to simulate snow surface temperature (Fig. 9). Rms errors of about 2 K were found for the new snow scheme integrations with the CdP datasets (see Fig. 9). These errors, which are believed to be related to the single-layer representation of snow in ISBA, could explain part of the 3–4-K rms errors shown in Figs. 10 and 11.

Another reason, which we would like to further discuss in the rest of this subsection, and which we believe could also be of importance to explain this lack of improvement, is related to the crude manner in which the model grid tiles snow cover fraction are determined in ISBA's snow models [fraction p_{sn}; see (1)–(3)]. For the stand-alone experiments described in section 3, this snow cover fraction did not play a significant role on the evolution of surface characteristics (including temperature) because measurements were taken over a small area, which could either be considered as completely snow covered or completely snow free ($p_{sn} = 0$ or $p_{sn} = 1$). For atmospheric models, in contrast, the representative area of each model grid point is very large, and accurate values for snow cover fraction are crucial for correctly calculating surface fluxes.

The role of snow cover fraction in the determination of surface fluxes is not direct in ISBA's snow models (for both old and new versions). In these snow schemes, which were qualified as belonging to a composite-layer type by Slater et al. (2001), surface temperature is provided by a single equation in which snow's thermal characteristics are blended with those of the snow-free portion of the model grid area. Thus, the ''effective'' surface fluxes used by the atmospheric model are not resulting from aggregation of surface fluxes over snow-covered and snow-free portions of model grid areas, but are rather the product of an effective temperature, which evolves according to the force–restore equation given in section 3 of Bélair et al. (2003).

As described in Yang et al. (1997) and Slater et al. (2001), snow cover fraction and snow albedo are closely connected in this type of model. Basically, surface albedo is larger for model grid tiles that are mostly covered with snow, as compared to model grid areas that are snow free. In this case of large surface albedo, less energy is available to warm the surface during daytime, which leads to lower surface temperature, smaller surface fluxes, and a weaker surface–boundary layer coupling. The snow cover fraction also influences the nighttime surface energy budget because of its emissivity, which is generally different from snow-free surfaces.

In ISBA's new snow package, the formulations for snow cover fraction over bare soil and vegetation were not modified and are the same as in ISBA's original snow package. The formulations given in (1) and (2) for p_{sng} and p_{snv} clearly reveal how simple the evaluation of snow cover fraction is in ISBA, and how it depends on quantities such as roughness length z_0 and parameter W_{cm}, which are either empirical or not well known.

More importantly, one should note that the total snow cover fraction p_{sn}, given in (3), critically depends on the vegetation fractional coverage, veg, which is another quantity that is not well known. For the relatively frequent case in which $p_{sng} \sim 1$ and $p_{snv} \sim 0$, that is, where there is enough snow to cover bare soil but not enough to cover the vegetation canopy, the total snow fraction is practically given by $p_{sn} \sim (1 - \text{veg})$. In the current regional weather forecasting system, the vegetation fractional coverage veg is specified in an empirical manner, using a correspondence table that makes the link between each vegetation type (provided by a land use classification) and the vegetation fractional coverage veg_i for all database pixels (1 km $\times$ 1 km). These pixels are then spatially averaged to produce the model grid scale veg field.

The correspondence between snow and vegetation fractional coverages is evidenced in Fig. 12. In this figure, snow cover fraction is relatively small (between 10% and 30%) along the boreal forest band where vegetation coverage fractions are about 90%. Conversely, snow fractions are larger over the American Midwest plains and over northern Canada.

To illustrate to what degree meteorological results are sensitive to snow cover fraction (which heavily depends on vegetation fractional coverage), an additional numerical integration was performed in which the vegetation fractional coverage was artificially decreased by 15%. (The decrease of vegetation fractional coverage was obtained by directly modifying the values in the correspondence table mentioned above.) This integration was initialized at 0000 UTC 15 March 2001. During that day, cloud-free skies were observed and predicted over most of Canada, and the associated large incoming solar fluxes at the surface provided optimal conditions for a maximum impact of surface processes on the evolution of the boundary layer.

Figure 13 shows the differences between this run's results and those from the control run, that is, with no decrease of the vegetation fractional coverage. The upper panel of this figure indicates that the 15% decrease of vegetation fractional coverage leads to, as expected, larger values of snow cover fraction p_{sn}. This increase of snow cover fraction is particularly significant over the boreal forest band (between 10% and 15%), because of the large vegetation fractional coverage and large SWE over this region.

Figure 13's lower panel reveals that the increase of snow cover fraction occurs in combination with lower surface air temperatures, at least for the 18-h forecast valid at 1800 UTC on 15 March 2001. From western Ontario to the eastern coast of Canada and the northeastern United States, temperature differences of the order of 1–1.5 K are found between the control and sensitivity runs. The vertical profiles shown in Fig. 14 reveal that this temperature difference is found for the whole depth of the boundary layer, which could be relatively deep, even in winter (about 500 m for the profiles in Fig. 14). It thus seems that an uncertainty of 15% on

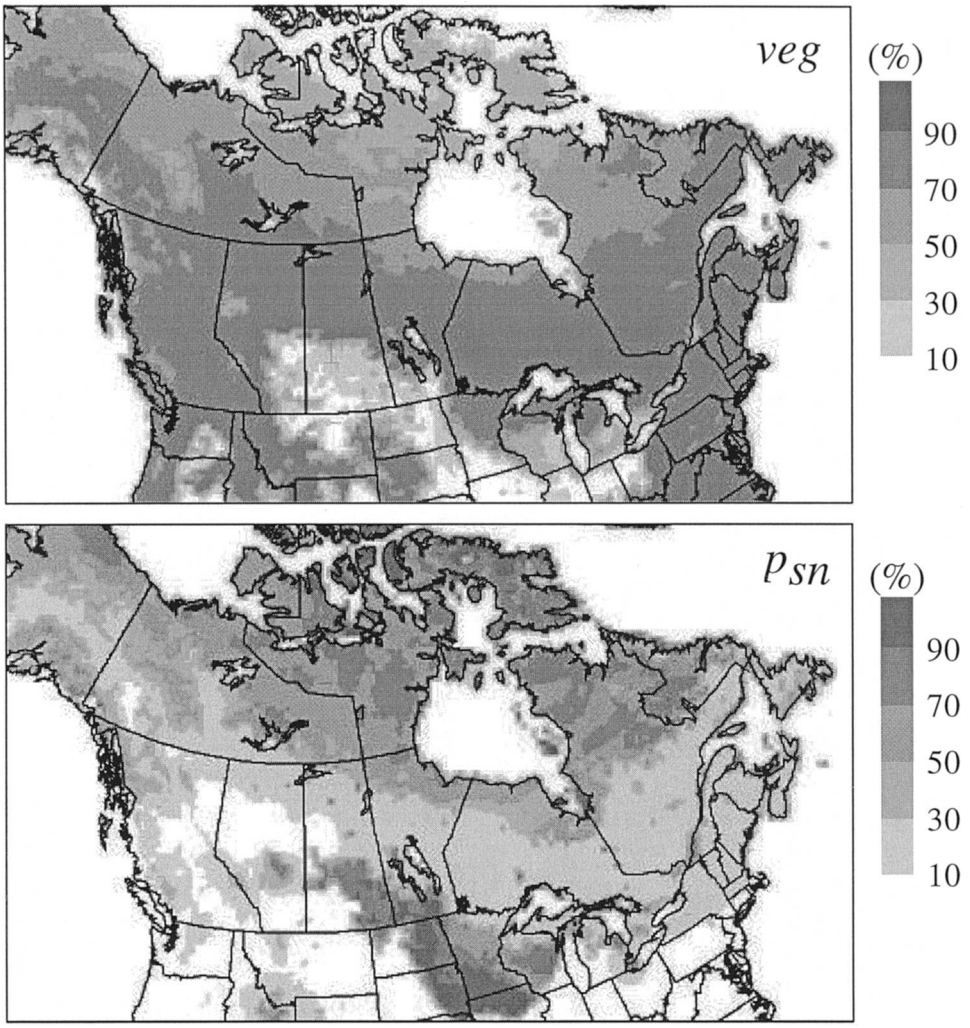

FIG. 12. Fraction of GEM's grid areas covered by (top) vegetation and (bottom), snow valid at 0000 UTC 15 Mar 2001.

the specification of vegetation fractional coverage could translate into uncertainties of about 10%–15% for the snow cover fraction, which in turn could be responsible for uncertainties of more than 1 K in the prediction of daytime maximum air temperature over snowy regions. This conclusion is troubling because our knowledge of snow and vegetation fractional coverages are probably not within 15% accuracy, especially in mesoscale atmospheric models (i.e., with a horizontal resolution of ~10–30 km) for which small-scale variability of vegetation is important. It is thus not inappropriate to believe that surface air temperature forecast errors associated with this problem could be as large as a few degrees, which is on the order of the rms errors presented in Figs. 10 and 11. This aspect of snow modeling is therefore of crucial importance and needs to be considered when including more sophisticated snow schemes in atmospheric models.

5. Summary and conclusions

This study examined the performance of a newly developed version of ISBA's snow scheme, which is based on a relatively simple representation of snow processes. Stand-alone verification tests showed that ISBA's new snow package was able to realistically reproduce the main characteristics of a winter snowpack (SWE and density) for two test sites at Col de Porte, France, and at Goose Bay, Newfoundland, Canada. SWE and snow density produced with the new scheme compared well with results obtained with CROCUS, a much more sophisticated multilayer snow model.

However, the modifications made to ISBA's snow scheme did not lead to improvement in snowmelt runoff and snow surface temperature. For snowmelt runoff, the results were quite similar for the three snow models examined. The differences in snowmelt runoff were

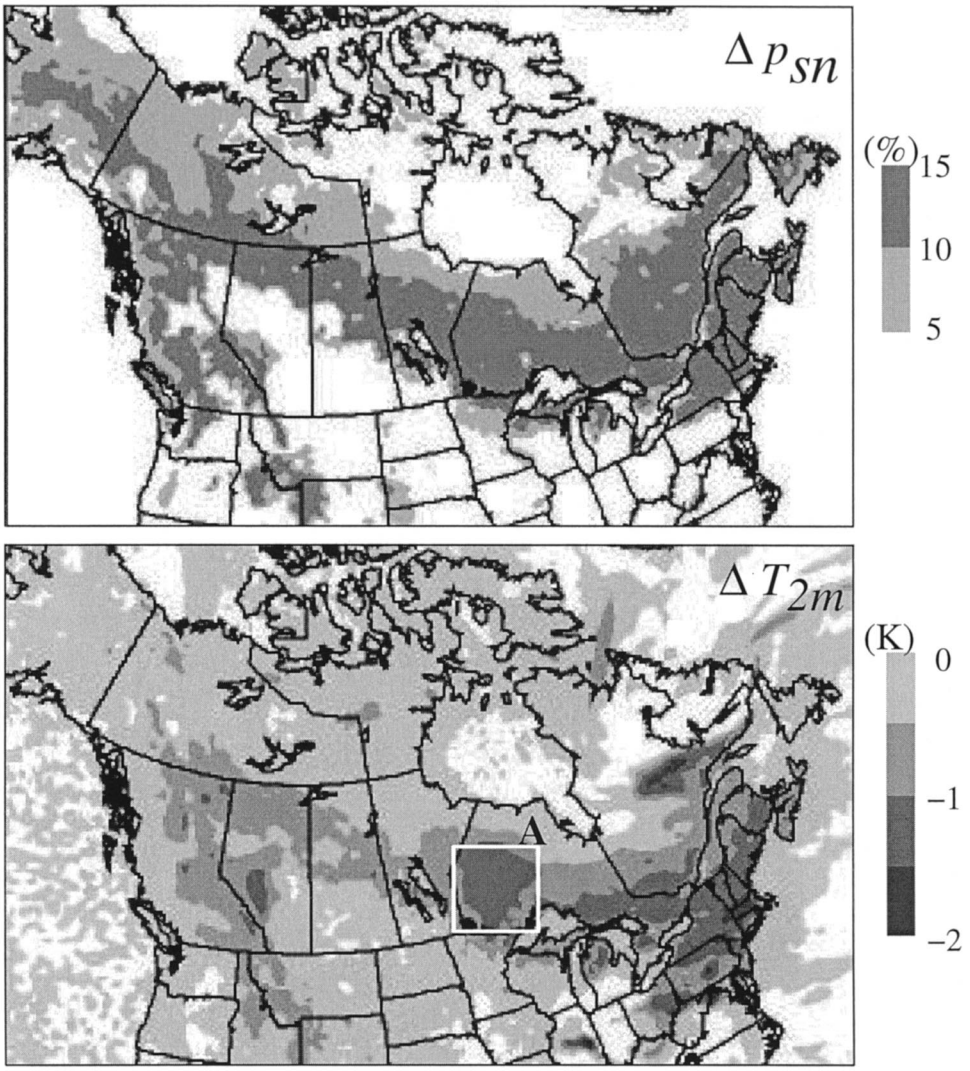

FIG. 13. Differences of (top) snow coverage fraction (p_{sn}; %) and (bottom) of low-level air temperature (T_{2m}; K) between a control and a sensitivity experiment (i.e., sensitivity − control) in which the vegetation fractional coverage is decreased by 15%. The differences were calculated for 18-h forecasts valid at 1800 UTC 15 Mar 2001. Region ''A'' shows the area for which the vertical profiles given in Fig. 14 were averaged.

small because of the dominant influence of atmospheric forcing (radiation, temperature, wind) for this quantity. For snow surface temperature, the two ISBA versions produced results that clearly did not compare as well against observations as CROCUS. We believe that the main reason for the much smaller rms errors for CROCUS is a better vertical representation of temperature and snow characteristics, which is not possible with the single-layer ISBA snow schemes. For example, the periodic daytime and nighttime thawing/freezing processes that occur near the snow surface, which are not well represented in a single-layer model, may have a significant influence on the surface temperature. This weak performance of ISBA's snow schemes for simulating snow surface temperature could be important because this temperature greatly influences the intensity of heat and water exchanges between snow and the overlying atmosphere.

The fully interactive preimplementation tests that were done with the Canadian regional weather forecast model indicate that replacing the highly parameterized snow model, which was previously used operationally at CMC, with ISBA's new snow scheme only had minor impacts on the model's atmospheric prediction. Objective evaluation against observations from surface stations and radiosondes for the northern (snow-covered) portion of North America for March 2001 showed that rms errors for low-level air temperature were slightly deteriorated with the new system, while the opposite was found for dewpoint depression. The signals for air

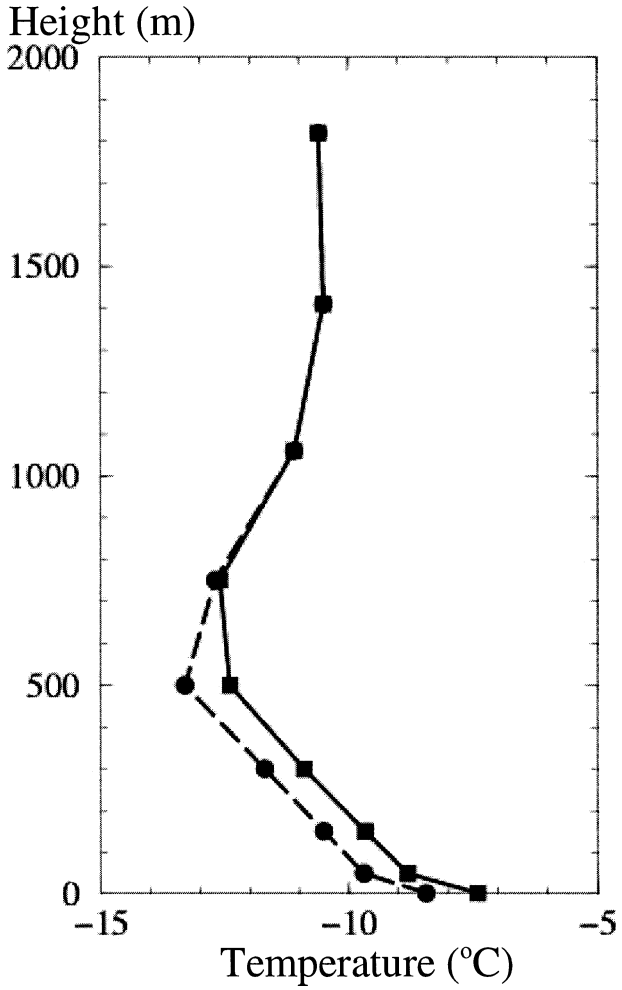

FIG. 14. Vertical profiles of temperature averaged over region A shown in Fig. 13 for a control (full line, squares) and a sensitivity (dashed line, circles) experiment in which the vegetation fraction is decreased by 15%. The vertical profiles were calculated using 18-h forecasts valid at 1800 UTC 15 Mar 2001.

temperature and dewpoint biases near the surface, on the other hand, were in contradiction for the two observational sets (surface stations and radiosondes).

Nevertheless, the objective scores clearly reveal that the impact of using the new snow scheme only occurs for a thin atmospheric layer above the surface, with not much effect on the numerical prediction of weather systems. For instance, quantitative precipitation forecasts were nearly unchanged by the inclusion of the new snow scheme. This is in contrast with the very positive results found in Bélair et al. (2003) for summertime precipitation, which was significantly improved by including ISBA into the regional weather forecasting system. This greater sensitivity of weather systems to surface fluxes is to be expected in summertime when greater coupling exists between the surface and the planetary boundary layer, due to large surface fluxes.

The lack of improvement (during the cold season) resulting from ISBA's operational implementation may seem surprising, considering how much more sophisticated this snow scheme is compared to its predecessor. This result is likely related, in part, to (i) the weak surface boundary layer that exist in winter, (ii) the use of the same snow mass fields as initial conditions, and (iii) the weak performance of ISBA's snow scheme for predicting surface temperature. The evaluation of the snow cover fraction for each of the atmospheric model's grid tiles was also shown to be a likely contributing factor. This snow cover fraction relies on simple formulations that depend on poorly known parameters like, for instance, vegetation fractional coverage, which is currently determined from vegetation-type databases in the current CMC operational suite. It was shown that uncertainties as small as 15% for the vegetation fractional coverage could be responsible for uncertainties as large as 1–1.5 K for near-surface and boundary layer temperatures. In other words, even the most sophisticated snow model, with a large number of snow layers and with a comprehensive treatment of snow processes such as snow settling, vapor transfers, metamorphism, etc., would not necessarily have a positive impact on atmospheric weather forecasting if the snow cover fraction of each model grid tile is not accurately specified. Because of this, one of our main objectives in the near future is to improve the representation of the snow cover fraction over bare soil and vegetation.

Acknowledgments. We would like to thank all those who were involved in the operational implementation of the new surface modeling and assimilation system at CMC. In the Meteorological Research Branch, Dr. Yves Delage participated to the elaboration of the surface modeling system. In the CMC development group, Louis Lefaivre, Gilles Verner, Judy St-James, and Normand Brunet greatly contributed to this implementation. In the CMC operation group, Garry Toth gave us a clearer view of the new system's impact on weather forecasting. We are thankful to Peter Schut and Brian Monette from Agriculture Canada for providing soil texture data over Canada. We also acknowledge Eric Martin, of Météo-France, for providing the Col de Porte data, and Météo-France for making the CROCUS model code available to this study. Finally, this work greatly benefited from the interactions between the first author and Dr. Joël Noilhan, Dr. Florence Habets, Dr. Aaron Boone, Dominique Giard, and Eric Bazile, all from Météo-France.

REFERENCES

Aguado, E., 1985: Radiation balances of melting snow covers at an open site in the central Sierra Nevada, California. *Water Resour. Res.,* **21,** 1649–1654.

Anderson, E. A., 1976: A point energy and mass balance model of a snow cover. NOAA Tech. Rep. NWS 19, 150 pp.

Barnett, T. P., L. Dümenil, U. Schlese, E. Roeckner, and M. Latif, 1989: The effect of Eurasian snow cover on regional and global climate variations. *J. Atmos. Sci.,* **46,** 661–685.

Bélair, S., L.-P. Crevier, J. Mailhot, B. Bilodeau, and Y. Delage, 2003: Operational implementation of the ISBA land surface scheme in the Canadian regional weather forecast model. Part I: Warm season results. *J. Hydrometeor.,* **4,** 352–370.

Blondin, C., 1989: Research on land surface parameterization schemes at ECMWF. *Proc. Workshop on Parameterization of Fluxes over Land Surface,* Reading, United Kingdom, ECMWF, 285–330.

Boone, A., and P. Etchevers, 2001: An intercomparison of three snow schemes of varying complexity coupled to the same land surface model: Local-scale evaluation at an Alpine site. *J. Hydrometeor.,* **2,** 374–394.

Brasnett, B., 1999: A global analysis of snow depth for numerical weather prediction. *J. Appl. Meteor.,* **38,** 726–740.

Brun, E., E. Martin, V. Simon, C. Gendre, and C. Coleou, 1989: An energy and mass model of snow cover suitable for operational avalanche forecasting. *J. Glaciol.,* **35,** 333–342.

——, P. David, M. Sudul, and G. Brunot, 1992: A numerical model to simulate snow-cover stratigraphy for operational avalanche forecasting. *J. Glaciol.,* **38,** 13–22.

Cohen, J., and D. Rind, 1991: The effect of snow cover on the climate. *J. Climate,* **4,** 689–706.

Douville, H., J.-F. Royer, and J.-F. Mahfouf, 1995: A new snow parameterization for the Météo-France climate model. *Climate Dyn.,* **12,** 21–35.

Ellis, A. W., and D. J. Leathers, 1999: Analysis of cold airmass temperature modification across the U.S. Great Plains as a consequence of snow depth and albedo. *J. Appl. Meteor.,* **38,** 696–711.

Essery, R., E. Martin, H. Douville, A. Fernandez, and E. Brun, 1999: A comparison of four snow models using observations from an alpine site. *Climate Dyn.,* **15,** 583–593.

Garen, D., D. Woodward, and F. Geter, 1999: A user agency's view of hydrologic, soil erosion and water quality modeling. *Catena,* **37,** 277–289.

Hahn, D. G., and J. Shukla, 1976: An apparent relationship between Eurasian snow cover and Indian monsoon rainfall. *J. Atmos. Sci.,* **33,** 2461–2462.

Idso, S. B., 1981: A set of equations for the full spectrum and 8–14 μm and 10.5–12.5 μm thermal radiation from cloudless skies. *Water Resour. Res.,* **17,** 295–304.

Jin, J., X. Gao, Z.-L. Yang, R. C. Bales, S. Sorrooshian, R. E. Dickinson, S. F. Sun, and G. X. Wu, 1999: Comparative analyses of physically based snowmelt models for climate simulations. *J. Climate,* **12,** 2643–2657.

Jordan, R., 1991: A one-dimensional temperature model for a snow cover. CRREL Special Rep. 91-1b, Cold Regions Research and Engineering Laboratory, Hanover, NH, 49 pp.

Loth, B., H.-F. Graf, and J. M. Oberhuber, 1993: Snow cover model for global climate simulations. *J. Geophys. Res.,* **98,** 10 451–10 464.

Mailhot, J., R. Sarrazin, B. Bilodean, N. Brunet, and G. Pellerin, 1997: Development of the 35-km version of the regional finite-element model. *Atmos.–Ocean,* **35,** 1–28.

——, and Coauthors, 1998: Scientific description of RPN physics library. Version 3.6, Recherche en Prévision Numérique, 188 pp. [Available from RPN, 2121 Trans-Canada, Dorval, QC H9P 1J3, Canada; also available online at http://www.cmc.ec.gc.ca/rpn/physic98.pdf.]

Manabe, S., 1969: Climate and the ocean circulation: 1. The atmospheric circulation and the hydrology of the earth's surface. *Mon. Wea. Rev.,* **97,** 739–805.

Marshall, S., J. O. Roads, and G. Glatzmaier, 1994: Snow hydrology in a general circulation model. *J. Climate,* **7,** 1251–1269.

Namias, J., 1985: Some empirical evidence for the influence of snow cover on temperature and precipitation. *Mon. Wea. Rev.,* **113,** 1542–1553.

Noilhan, J., and S. Planton, 1989: A simple parameterization of land surface processes for meteorological models. *Mon. Wea. Rev.,* **117,** 536–549.

Pitman, A. J., Z. L. Yang, J. C. Cogley, and A. Henderson-Sellers, 1991: Description of bare essentials of surface transfer for the Bureau of Meteorology Research Centre AGCM. BMRC Research Rep. 32, BMRC, Melbourne, Australia.

Schlosser, C. A., and Coauthors, 2000: Simulations of a boreal grassland hydrology at Valdai, Russia: PILPS phase 2(d). *Mon. Wea. Rev.,* **128,** 301–321.

Segal, M., C. Anderson, R. W. Arritt, R. M. Rabin, and D. W. Martin, 1999: Some observations of the clearing of cumulus clouds downwind from snow-covered areas. *Mon. Wea. Rev.,* **127,** 1687–1692.

Sellers, W. D., 1965: *Physical Climatology.* University of Chicago Press, 272 pp.

Slater, A. G., A. J. Pitman, and C. E. Desborough, 1998: Simulation of freeze–thaw cycles in a general circulation model land surface scheme. *J. Geophys. Res.,* **103,** 11 303–11 312.

——, and Coauthors, 2001: The representation of snow in land surface schemes: Results from PILPS 2(d). *J. Hydrometeor.,* **2,** 7–25.

Sun, S., J. Jin, and Y. Xue, 1999: A simple snow–atmosphere–soil transfer model. *J. Geophys. Res.,* **104,** 19 587–19 597.

Tabler, R. D., C. S. Benson, B. W. Santana, and P. Ganguly, 1990: Estimating snow transport from wind speed records: Estimates versus measurements at Prudhoe Bay, Alaska. *Proc. 58th Annual Meeting of the Western Snow Conf.,* 61–78.

Verseghy, D. L., 1991: CLASS—A Canadian land surface scheme for GCMs. I. Soil model. *Int. J. Climatol.,* **11,** 111–133.

Viterbo, P., and A. K. Betts, 1999: Impact on ECMWF forecasts of changes to the albedo of the boreal forests in the presence of snow. *J. Geophys. Res.,* **104,** 27 803–27 810.

Walsh, J. E., W. H. Jasperson, and B. Ross, 1985: Influences of snow cover and soil moisture on monthly air temperature. *Mon. Wea. Rev.,* **113,** 756–768.

Yang, Z.-L., R. E. Dickinson, A. Robock, and K. Y. Vinnikov, 1997: Validation of the snow submodel of the Biosphere–Atmosphere Transfer Scheme with Russian snow cover and meteorological observational data. *J. Climate,* **10,** 353–373.

Yen, Y., 1981: Review of thermal properties of snow, ice, and sea-ice. CRREL Rep.